PERGAMON

Journal of Structural Geology 21 (1999) 479–492

JOURNAL OF STRUCTURAL GEOLOGY

Marked along-strike variations in dip of normal faults—the Lokichar fault, N. Kenya rift: a possible cause for metamorphic core complexes

C.K. Morley

Department of Petroleum Geoscience, University of Brunei Darussalam, Bandar Seri Begawan, 2028, Negara, Brunei

Received 5 May 1998; accepted 16 November 1998

Abstract

The Lokichar fault is a major boundary fault in the northern Kenya rift, mapped from seismic reflection data. The fault is a mixture of high 45–60°, low 20–45° and very low (12–20°) angle segments. The areas of least displacement (up to a maximum 10 km heave) are the very low-angle fault segments (12–20°). The southern higher angle fault segment has a maximum estimated heave of about 20 km. Initiation of normal faults at a low angle cannot be easily explained by rock mechanics theory. Common explanations for such faults include: (1) rotation of higher angle faults by the domino faulting model, (2) rotation of large-displacement faults by isostatic instability created by the faulting (rolling hinge models), and (3) reactivation of low-angle pre-existing fabrics. The Lokichar fault geometry is inconsistent with any of the above explanations. The very low-angle segments coincide with regions of intense igneous intrusive activity. Re-orientation of the stress axes from the simple Andersonian condition, could permit normal faults to form at a lower angle; this may happen around intrusive complexes or by setting up a basal shear stress between flowing and static crust. If faults associated with metamorphic core complexes were associated with marked along-strike changes in fault angle the resulting variations in footwall uplift could give rise to the antiformal metamorphic core complex geometry.

1. Introduction

Seismic reflection data across the East African rift shows most major boundary faults are high-angle (45–70°, e.g. Ebinger et al., 1987; Rosendahl et al., 1988; Dunkleman et al., 1989; Morley, 1989). Seismic reflection data acquired by Amoco P.C. in the northern Kenya rift have revealed several large faults imaged on the East African seismic data that are very low-angle (12–20°). These faults are exceptions rather than the rule; however their unusual occurrence must be explained. The best imaged low-angle fault is the Lokichar fault in northern Kenya which is described below. This paper examines some of the implications of the Lokichar fault for the origin of low-angle normal faults, and models that have been developed to explain the origin and motions on low-angle normal faults elsewhere in the world.

1.1. Geometry of the Lokichar fault

The Lokichar fault is the boundary fault to a large half graben in the southern Turkana area (Morley et al., 1992; Fig. 1). Nineteen dip seismic lines and three strike lines provide control on the Lokichar fault geometry to about 4 s two way travel time, or depths of 8–10 km, over a strike distance of 140 km (Figs. 2–6). Crystalline basement forms the footwall, whilst the rift basin, floored by crystalline basement, forms the hang-

E-mail address: chris@ubd.edu.bn (C.K. Morley)

0191-8141/99/$ - see front matter
PII: S0191-8141(99)00043-7

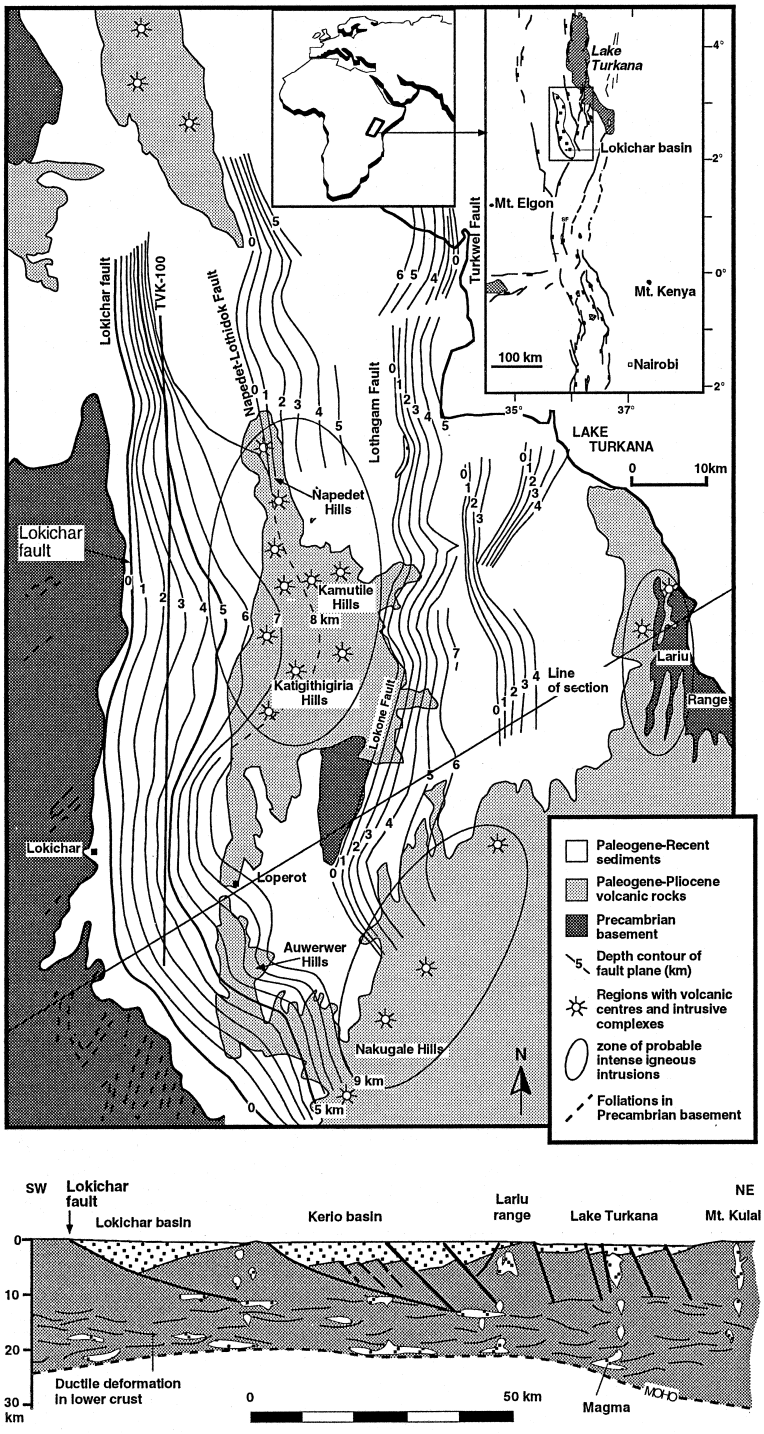

Fig. 1. Regional map showing maps of major fault planes from seismic reflection data, western Turkana area of northern Kenya. The locations of major igneous intrusive complexes are inferred from the identification of volcanic centers in surface outcrops.

ing wall. The termination of reflectors from the rift basin provides a fairly precise marker for the location of the boundary fault. Where the fault plane lies entirely in basement, many seismic lines display reflections that appear to be from the fault plane. The surface trace of the fault, marked by the edge of Precambrian basement outcrops, coincides well with the fault defined on seismic data.

Fig. 1 shows the location of several half graben-bounding faults in the area. These faults are thought

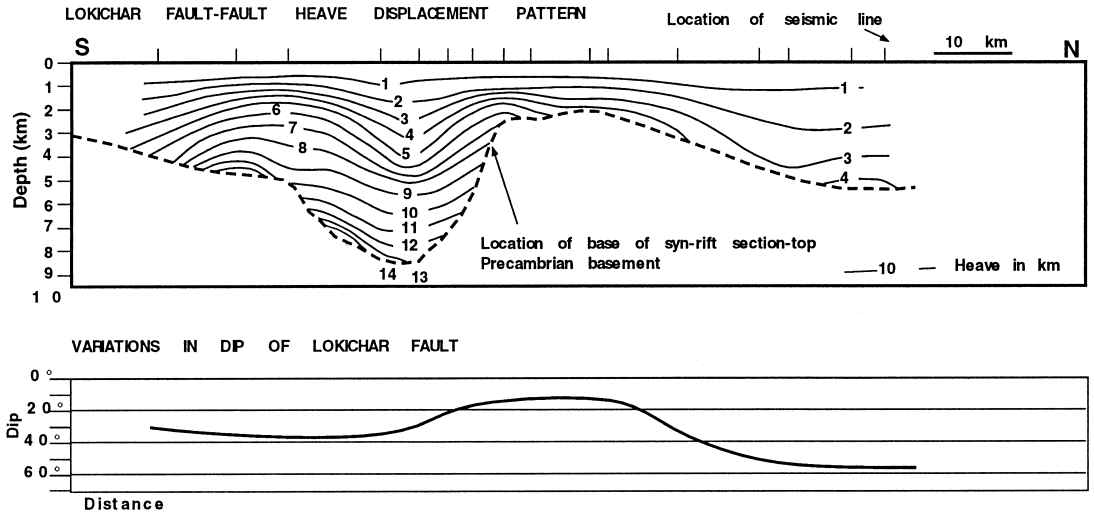

Fig. 2. Map of Lokichar fault plane made from seismic reflection data (see Fig. 1 for location). The horizonal axis is distance along the strike of the fault. The thick line at the base of the heave contours marks the base of the syn-rift section-top of Precambrian basement, and represents the vertical throw. The contours above represent the horizontal extension or heave on the fault plane, which increases with depth, as mapped from the displacement of the hanging wall basin fill reflections with respect to the present outcrop of the fault. This is actually a minimum estimate because footwall uplift has not been taken into account.

to pass independently into a mid-crustal brittle–ductile transition zone, and not form part of a linked detachment system (Hendrie et al., 1994).

Mapping of the fault plane shows the following features:

1. In general the fault plane is planar, although in the area of line 102W it has a listric shape.
2. The fault plane changes dip considerably along strike from about 12° to 60° (Figs. 2 and 3).
3. The southern portion of the fault is curved in map view, but planar in cross-section; the curvature is accompanied by the fault changing dip along strike (Figs. 1 and 4).
4. The fault displacement changes considerably along strike. Using the top of the Precambrian basement–base syn-rift section as a marker there are two areas of relatively high throw, most pronounced is the southern area which displays up to 8 km throw and 13–15 km heave (Figs. 2 and 4), separated by a central area of low displacement (about 2 km throw and 4–5 km heave). The fault dip is higher in the areas of high displacement and considerably lower in the areas of low displacement. The method for measuring displacement is discussed below.

The top of the Precambrian basement–base syn-rift reflection is generally well defined on seismic lines. The offset of this reflection from the surface outcrop of the fault trace provides an approximate estimate of the displacement on the fault (Fig. 4). The footwall of the fault is Precambrian basement, hence no marker horizons within the Tertiary basin fill can be tied to the footwall. The extension estimates (Figs. 2 and 4) underestimate the actual extension to some extent because the footwall area has been eroded during the late Tertiary.

Hendrie et al. (1994) used a flexural cantilever model to estimate the amount of footwall uplift and erosion for the Lokichar fault. In general this model predicts footwall uplift is larger for high-angle faults rather than low-angle faults, and where the basin fill density contrast with basement is greatest (Kusznir et al., 1991). Hence the area of maximum basin fill and highest fault dip, both of which coincide in the Lokichar basin, should have the highest footwall uplift. Similarly the area where the boundary fault is low-angle coincides with a thinner basin fill, indicating relatively low footwall uplift. Measuring displacement from the surface trace of the fault to the hanging wall cutoff may underestimate heave along the Lokichar fault by a maximum of about 5 km (Hendrie et al., 1994). For the low-angle portion of the fault similar modeling suggests displacement may be underestimated by a maximum of 1.8 km (Fig. 5). Thus in relative terms the displacement pattern remains the same, since the maximum underestimate of extension occurs on the steepest-dipping portion of the fault and is least for the gently-dipping sections of the fault.

The top Precambrian basement reflection in general provides a good indication of the maximum displacement on the Lokichar fault in the brittle upper crust. The main way to add extra extension to the fault below the top of Precambrian basement would be for hanging wall faults to sole into the Lokichar fault. There are, however, relatively few minor faults imaged

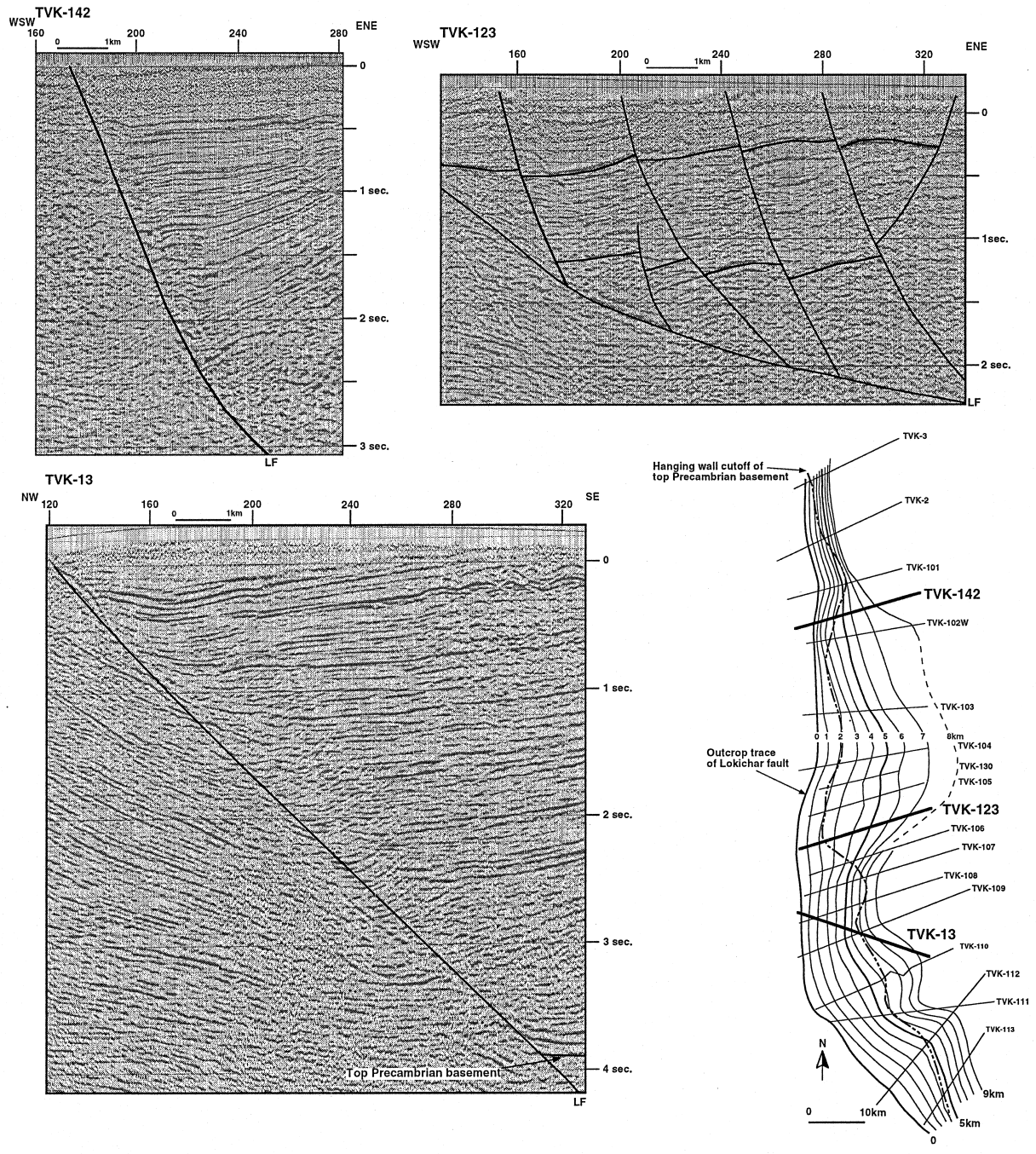

Fig. 3. Examples of Lokichar fault plane geometry on seismic reflection data; the fault plane used for locations can be seen in Figs. 1 and 4.

on seismic reflection data that could contribute significant amounts of extension to the Lokichar fault downdip of the top-of-basement hanging wall cutoff (Fig. 6). Significantly, however, more minor faults occur in the area of the low-angle Lokichar fault segment, than the high-angle segments. These minor faults could contribute an extra 2–3 km heave to the low-angle portion of the boundary fault, below the hanging wall cutoff of the top Precambrian basement. Consequently estimates of the maximum heave on the low-angle fault segment lie in the region of 8–10 km, while for the southern high-angle segment maximum heave is 18–20 km.

Fault geometry in rifts has been the subject of considerable debate in the literature (e.g. Gibbs, 1983; Wernicke, 1985; Jackson, 1987; Buck, 1988; Lister and Davis, 1989; Kusznir et al., 1995). Are faults dominantly listric or planar in cross-section? Are they in-

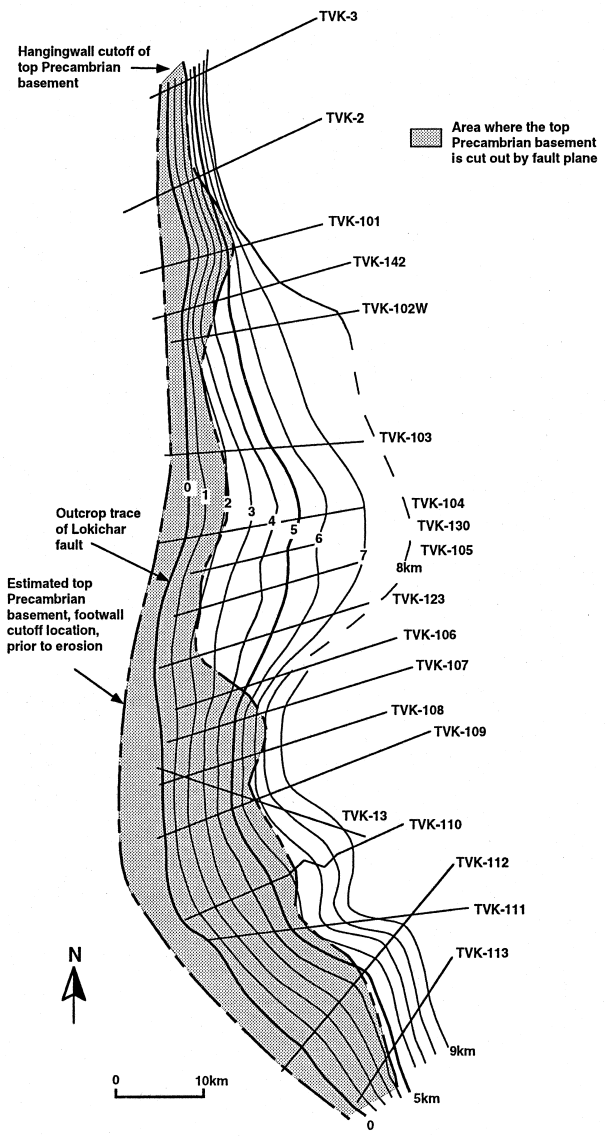

Fig. 4. Structure contour map on the Lokichar fault plane. An estimate of the location of the top of basement footwall cutoff prior to erosion was made based on the STRETCH model (Kusznir et al., 1991). (See Fig. 1 for location.)

itially high-angle or low-angle? What are the mechanisms for causing such changes in fault geometry? The Lokichar fault demonstrates that over a distance of 150 km, a single fault passes from a high-angle planar geometry to intermediate and low-angle planar geometries, and in one area has a listric geometry. This has considerable implications for the normal fault models which maintain that low-angle faults develop in response to different boundary conditions than high-angle faults (e.g. Buck, 1988; Yin, 1989). Whilst this may still be true, to explain the Lokichar fault, it is necessary to find some very local changes in such conditions.

1.2. Timing of deformation along the Lokichar fault

In western Turkana the Tertiary syn-rift basin fill overlies crystalline Precambrian basement. Seismic data show pronounced expansion of the mixed sedimentary and volcanic syn-rift section towards the Lokichar fault. There is no indication of any pre-rift sedimentary section.

There are two depocenters along the Lokichar fault separated by a central antiformal high or transverse anticline (Fig. 6, strike section TVK-100). The southern depocentre is called the Lokichar basin and the northern depocentre is the North Lokichar basin. Correlation of seismic reflection data across the basins shows that the west-thickening Lokichar basin fill underlies the west-thickening North Lokichar basin. Underlying the west-thickening half graben fill in the North Lokichar basin is an east-thickening reflection package that can be tied at the surface to seismic reflection data in the vicinity of the Lothidok hills. The surface outcrops have been described as a succession of volcanics and volcani-clastics of late Oligocene–middle Miocene age by Boschetto et al. (1992) (Fig. 7).

The basin fill in the hanging wall of the Lokichar fault is dated as latest Oligocene–middle Miocene from palynology, vertebrate fossils and radiometric age dates of lava flows from suface outcrops and shallow boreholes (Morley et al., 1992). These ages were confirmed by data from an exploration well (Loperot-1) drilled by Shell (Morley et al., in press). Tentative dating of the lowest sequence in the well, not seen in outcrop, points to a possible late Eocene–early Oligocene age (Fig. 7).

The North Lokichar basin is dated by correlation of seismic reflection data with surface outcrops. The west-thickening basin fill overlies middle Miocene volcanic units and is of late Miocene–Pliocene age (Morley et al., 1992).

The picture that emerges from the basin geometries described above is that the west-thickening Paleogene–mid Miocene Lokichar basin passed northwards into an east-thickening basin (Lothidok basin). In the vicinity of the present day transverse anticline or saddle area (Figs. 6 and 7), the displacement on the east-dipping Lokichar fault was transferred via a convergent overlapping transfer zone (Morley et al., 1990) to the (inferred) west-dipping boundary fault of the Lothidok basin.

The subsequent development of the North Lokichar basin beginning in the late Miocene could represent northerly propagation of the original Lokichar fault. Alternatively a new boundary fault may have formed along strike of the Lokichar fault and propagated south to link with it. Linkage occurred around the

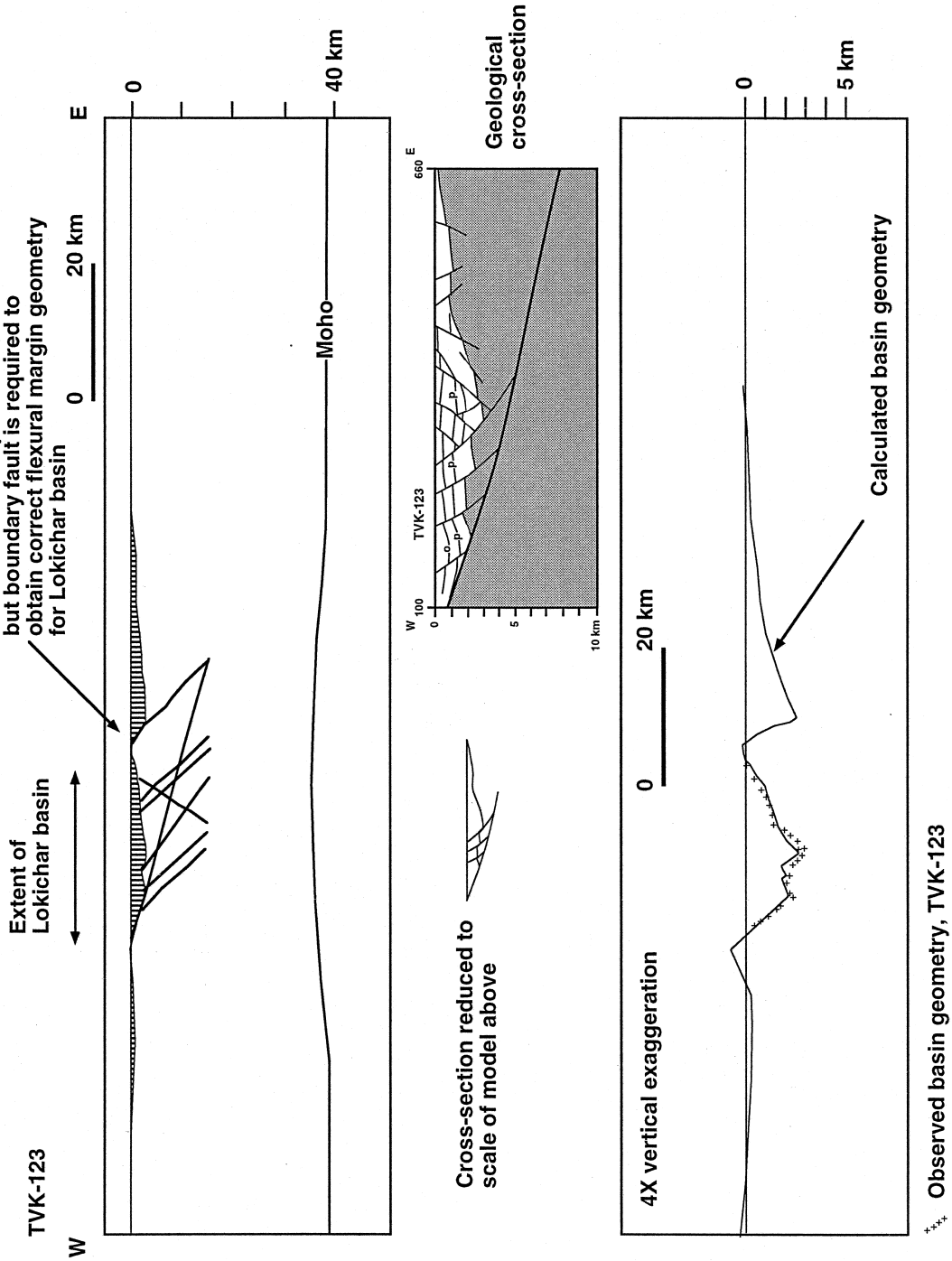

Fig. 5. Stretch model for line TVK-123, Turkana area, Kenya (see Fig. 4 for location). The model involved 5 km extension on a fault of 25° initial dip, and an effective elastic thickness (Te) of 3 km.

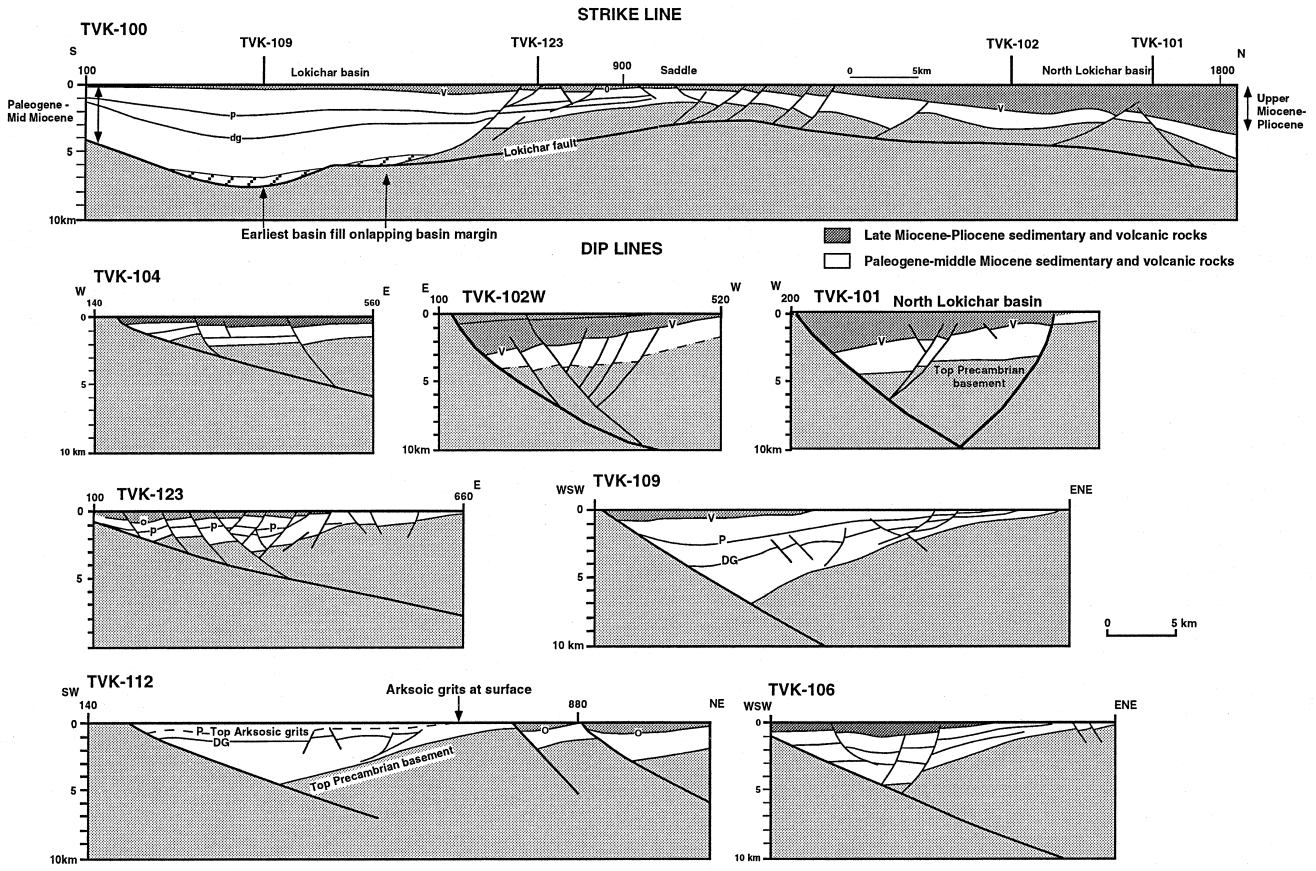

Fig. 6. Strike and dip cross-sections across the Lokichar basin based on seismic reflection data. The fault plane used for locations can be seen in Fig. 4. The strike-section is based on strike seismic line TVK-100. It illustrates the two separate depocenters created at different times, with a very deep Paleogene–middle Miocene depocenter in the south (white) and an upper Miocene–Pliocene depocenter in the north (grey) separated by a high area.

low-angle portion of the Lokichar fault in the central area.

In detail there are several features which point to a more complex history of motion on parts of the Lokichar fault. On two lines only (TVK 107 and 106) there is evidence of minor Pliocene inversion, as indicated by a hanging wall fold.

1.3. Origin of low-angle faults

Since the recognition of low-angle normal faults in the Basin and Range, there have been questions raised as to how such faults are mechanically possible, whether they could represent rotated high-angle faults (Proffett, 1977), and whether they are applicable to tectonic settings outside of abnormally hot, thick continental crust (see Lister and Davis, 1989; Wernicke, 1995; Wills and Buck, 1997).

Isostatic rotation of initially high-angle normal faults to lower angles has been invoked to explain the mechanical problems of initiating the detachment faults as low-angle faults (e.g. Wernicke and Axen, 1988; Buck, 1988). However, field evidence has revealed some late low-angle faults that are geometrically consistent with mapped bedding and truncations of high-angle faults only when they were initiated at a low angle (e.g. Whipple detachment fault, Lister and Davis, 1989; Yin and Dunn, 1992; Rawhide fault, Scott and Lister, 1992).

Since the field evidence for at least some initially low-angle faults is strong, some workers have argued that the assumption of Andersonian fault mechanics (one of the principal stress axes is vertical, Anderson, 1951) is not necessarily correct (Lister and Davis, 1989; Yin, 1989; Parsons and Thompson, 1993). In order to generate low-angle faults it is necessary to find a mechanism which will cause rotation of the vertical principal stress direction. Such non-Andersonian conditions may be caused by a basal shear stress, such as regional ductile flow in the lower crust or between the crust and the mantle (Yin, 1989; Lister and Davis, 1989), or by igneous intrusion (Parsons and Thompson, 1993).

Once a low-angle normal fault is formed, there still remains the problem of why the fault should remain active. If a vertical σ_1 is resolved into normal and

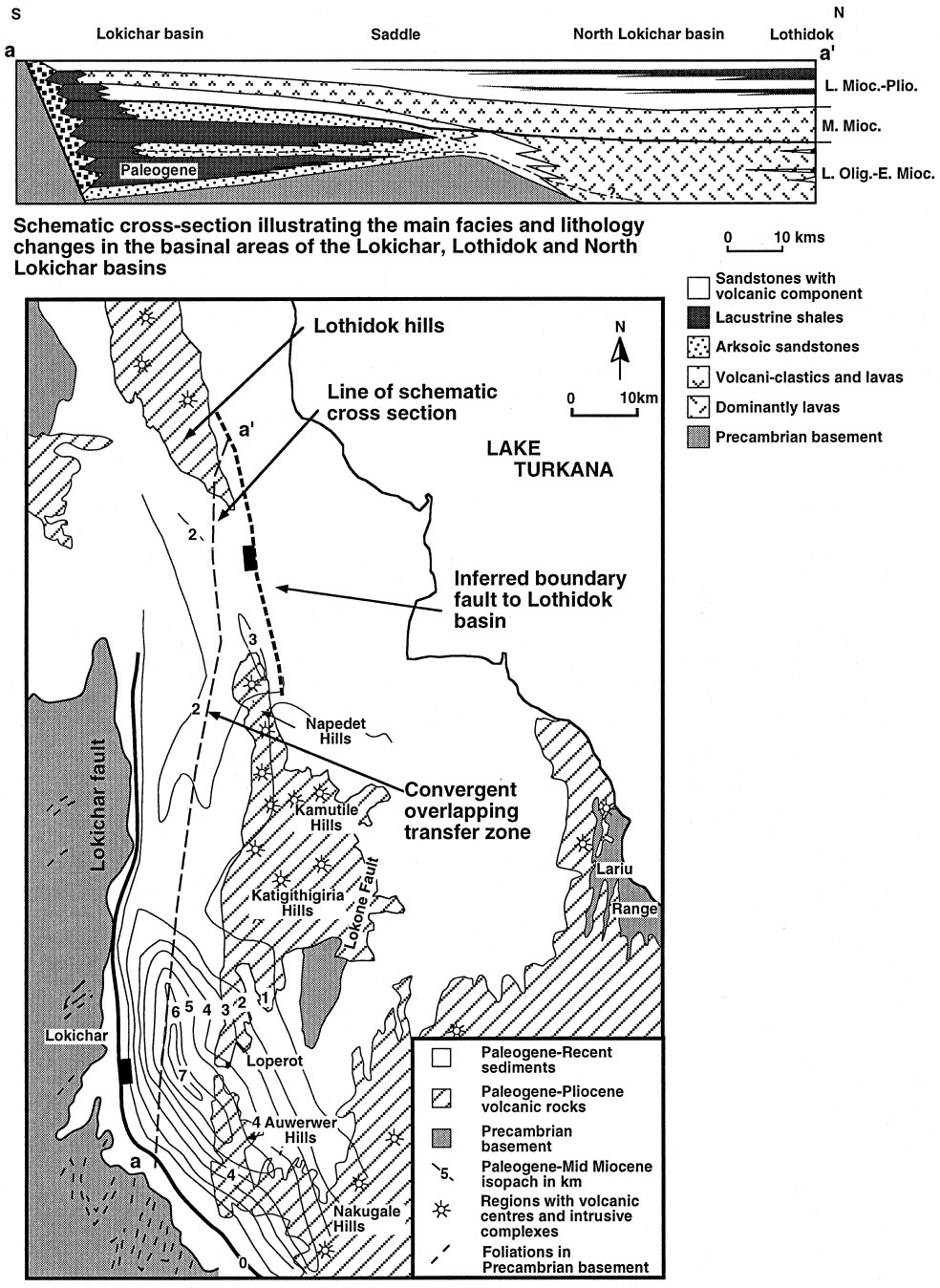

Fig. 7. Stratigraphic setting for the Lokichar basin. The schematic stratigraphic cross-section illustrates the marked change from basement-derived sediments in the Lokichar basin to volcanic-dominated basin fill in the Lothidok area. The map illustrates the isopach pattern for the Paleogene–middle Miocene section, thicknesses are given in kilometers.

shear components then normal stress becomes increasingly larger with respect to shear stress as the fault dip becomes lower (e.g. Byerlee, 1978). For a typical friction coefficient between 0.5 and 1, normal faults dipping less than 30–40° are predicted to lock up. This is supported by modern seismicity studies of active normal fault systems which fail to show active low-angle faults (e.g. Jackson, 1987; Doser and Yarwood, 1994). Hence it is difficult to understand how, under Andersonian conditions, it is possible for low-angle normal faults to be active, although high pore fluid pressures may help (e.g. Axen, 1992).

The Lokichar fault has the following characteristics:

1. A major relatively high angle (30–50°) fault passes along strike, into a low-angle fault segment (12–20°) over a distance of 50 km. Hence fault geometry can change considerably along-strike.

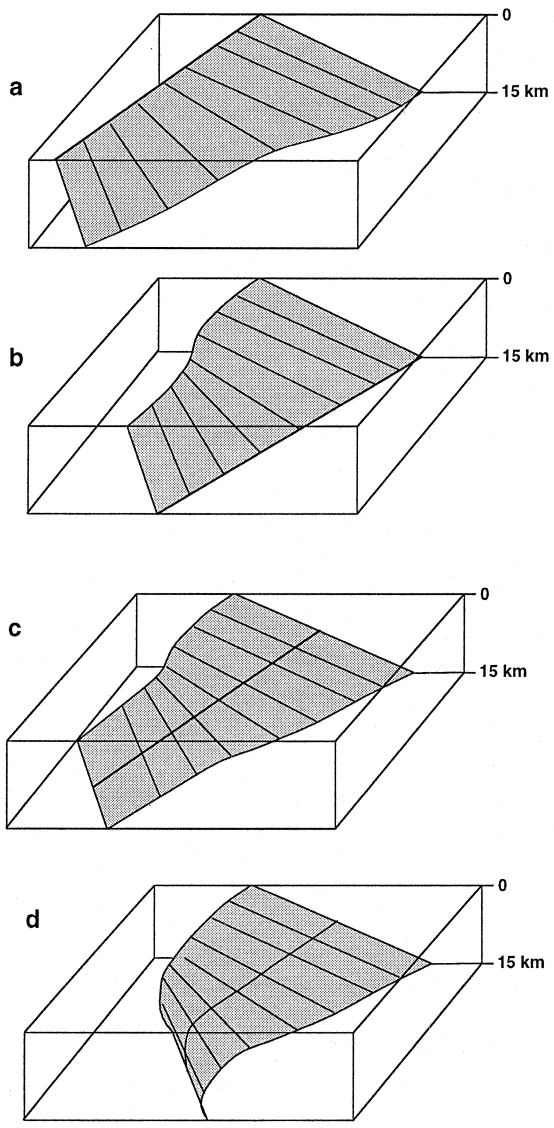

Fig. 8. Schematic illustration of how a fault which appears planar in cross-section can display curved map view geometries due to lateral variations in dip of the fault plane. (a) Straight surface map trace, curved base, (b) straight base, curved surface map trace, (c) curvature of both the base and surface fault trace, the straight segment lies mid way along the fault, (d) laterally curving fault and variable fault angle.

2. The low-angle fault segments are not representative of highly extended and rotated high-angle faults, but actually coincide with areas of least displacement. Depositional lows coincide with fault segments of higher angle, and the half graben stratigraphy thins towards the low-angle fault segments. Keeping other critical parameters similar, isostatically-induced rotation of the fault plane should occur along the high-angle, high-displacement portions of the fault (Buck, 1988; Kusznir et al., 1995). Consequently the observed displacement geometries are completely the reverse of those expected if the low-angle fault segment of the Lokichar fault was the result of isostatic rotation of an initially high-angle fault.
3. The Lokichar fault cross-cuts folded foliations in Precambrian basement at a high angle, hence there is no influence from pre-rift fabrics (Fig. 1).
4. The Lokichar fault appears to be predominantly planar in cross-section. For the fault to change angle along strike, but maintain a linear outcrop trace, would require the base of the fault (where it passes into the brittle–ductile transition zone) to form a salient (Figs. 4 and 8a). If the base of the fault is linear (Fig. 8b) then the outcrop trace of the fault should be curved. Intermediate geometries can also occur (Fig. 8c). Alternatively more complex, laterally curving geometries may develop (Fig. 8d); such is the case for the southern portion of the Lokichar fault.

The Turkana area is an atypical part of the Kenya rift. It is 2–3 times wider than most parts, has a Paleogene history and a long history of extensive volcanism. It is an area of high extension (perhaps 40 km, Hendrie et al., 1994). Other parts of the rift (e.g. Lake Tanganyika) display high-angle boundary faults (60–70°) and a maximum of about 10–14 km regional extension (Morley, 1989; Kusznir et al., 1995).

1.4. Potential role of magma in formation of low-angle faults

Parsons and Thompson (1993) have discussed the role that mid-crustal igneous intrusions might play in initiating low-angle normal faults. They proposed that if the intrusions inflate the crust locally at a rate faster than tectonic extension, then intense extensional stress would be located above the zone of intrusions. The overpressured magma may be intruded in sufficient quantities to locally create compressional conditions (Rubin and Pollard, 1988). Under such circumstances the maximum principal stress direction will tend to be rotated from a vertical orientation near the surface to horizontal approaching an intrusive complex. In addition large intrusive complexes could locally raise the geothermal gradient, thereby weakening the upper crust and reducing the differential stress that could be supported.

Re-orientation of the principal stresses could permit normal faults to be initiated at lower angles than predicted by the simple Andersonian model. The faults would have to be initiated during the period of magmatic intrusion and remain as planes of sufficient weakness to be reactivated once the anomalous stress conditions were dissipated.

Ductile flow of the lower crust (possibly induced by magmatic heating) could also create asymmetric

boundary conditions favorable to the formation of low-angle normal faults (Yin, 1989). Defending this model, Yin (1990) proposed that the shear strength of the crust at a depth of 10 km could be as low as 11–21 MPa if high pore fluid pressure ratios (0.8–0.9) were present. Igneous activity is one means by which such high pore fluid pressures could be temporarily attained.

There are some thermal and deep crustal data to support the applicability of the ductile flow model of Yin (1989) to the Lokichar fault. Sparse heat flow data indicate high crustal temperatures today, several million years after extension was last active in the area. Values are likely to have been higher in the past when the rift was active. Two exploration wells in western Turkana yielded geothermal gradients of 3.1°C/100 m and 4.2°C/100 m (Morley et al., in press). For the hottest well a heat flow of 80 mW/m^2 has been estimated (Le Van Hung, 1996). Seismic refraction data indicates northwards crustal thinning of a 6.8 km/s layer, which lies immediately above the crust–mantle transition, from a thickness of 9 km in the southern rift to 2 km in the Turkana area. This thinning could be explained by significant ductile flow of the lower crust (Mechie et al., 1994).

One final possibility is that the intrusions first cause compression (e.g. Skarmeta and Price, 1984) that leads to the formation of low-angle thrust faults. Subsequent normal fault activity then reactivates these low-angle pre-existing fabrics (which cannot be seen in the surface geology).

1.5. Timing of deformation and magmatism

When trying to relate magmatic intrusions to fault orientations in the Kenya rift, it is necessary to match the timing of faulting and igneous activity and to correlate lateral changes in fault activity with the exposed igneous rocks (Fig. 1). There are numerous flows in the Napedet, Kamutile, Kathigithigiria, and Auwerwer Hills dated from 15 to 12 Ma. Volcanic centers and pipes are largely confined to the northern part of the area, coincident with the lowest-angle segment of the Lokichar fault plane (Fig. 1).

If the intrusives did influence the fault geometry, there is a problem of timing. The fault system was initiated in the Paleogene, whilst the known igneous dykes, plugs and extrusives are of middle Miocene age. If the Paleogene fault system was influenced by intrusives then it is necessary to infer their existence based on the geometry of the Lokichar fault alone. There was extensive volcanism of this age in Lothidok Hills, just to the north of the Lokichar basin (Boschetto et al., 1992). Forty kilometers to the east of the Napedet Hills a date of 32 ± 3.8 Ma was obtained from a dyke at the northern end of the Lariu Range (Morley et al., 1992). So although no late Oligocene–early Miocene surface volcanism is present in the Lokichar basin, it is possible that intrusive volcanic rocks of this age extended south, some 30–40 km beyond the present day surface outcrops.

Alternatively if the present fault geometry is related to the known episode of volcanism, then it could only have been formed during the middle Miocene. This would imply that an older, high-angle fault system was replaced by the low-angle fault system once the intrusive complexes were emplaced. The sector of lowest fault dip, between lines TVK-123 and 102W, displays reduced expansion of pre-middle Miocene section into the boundary fault. There is, however, expansion of section into secondary faults in the hanging wall of the detachment. Hence it can be argued that the early high-angle faults represent minor faults associated with a hinged margin, or splays of the Lokichar fault. The high-angle faults have subsequently been truncated by the low-angle fault.

The gradational nature of the transition to lower angle dips along the Lokichar fault argues against the low-angle segment forming late, as does the limited expansion of late Miocene–Pliocene section into the low-angle fault segment, and the weak but relatively more pronounced expansion of the older section into the fault south of TVK 103. Consequently the low-angle segment is thought to be an early feature.

Other major faults in the Turkana area can also be mapped and appear to show similar characteristics where faults decrease in dip approaching regions with volcanic centers (Fig. 1). The Napedet–Lothidok Hills fault decreases in dip approaching the Napedet Hills and the Lokhone Fault decreases in dip approaching the Nakugale Hills.

1.6. Problems with models for principal stress rotation

The models for principal stress rotation have been recently reviewed by Wills and Buck (1997) who posed the question: can these models generate sufficient shear stresses to cause motion on low-angle faults? They concluded that under most geologically reasonable conditions, motion would occur on high-angle normal faults rather than on low-angle faults.

One scenario where Wills and Buck (1997) could obtain motion on low-angle faults was for a cohesionless fault in a zone of very high (almost lithostatic) pore fluid pressures, with the pore fluid pressures being lower both above and below the fault. While such conditions exist for mobile shale tectonics associated with deltas, it is more difficult to understand how such conditions could develop and be sustained in crystalline basement. However one possibility is the elevation of pore fluid pressures by the arrival of magma-related volatile fluids from depth. These overpressured fluids

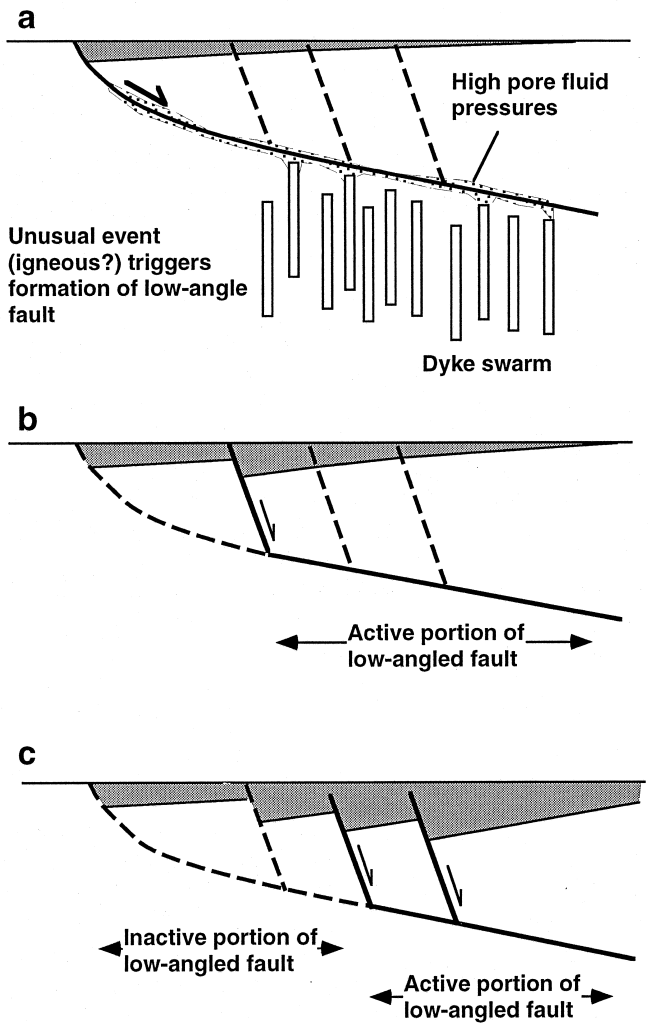

Fig. 9. Illustration of the evolution of a hypothetical low-angle fault. (a) Intitiation of low-angle fault trace. (b) and (c) Mechanical difficulties of moving the entire low-angle segment favor motion on higher angle domino faults, and reactivation of only a portion of the low-angle fault trace.

could rise in pipes or dykes through lower-pressured rocks. Their arrival at a major normal fault zone may trigger motion and seismic pumping on that fault zone, thus avoiding transmission of higher pore fluid pressures to the hanging wall. Hence a series of transient, magma-related high pore-fluid pressure events might satisfy the conditions for low-angle fault displacement required by Wills and Buck (1997). The current state of exposure in northern Kenya does not, however, permit the necessary observations of the deeper parts of the fault zone to be made. Minor faults are exposed at the surface that are intruded by dykes, which have 1–2 cm mineral veins (barytes, calcite) with slickensides on their margins.

The presence of numerous high-angle faults in the hanging wall of the low-angle fault segment strongly supports the finite element models of Wills and Buck (1997) that indicate high-angle faults should dominate the deformation style. The low-angle fault segment may not have reactivated along its entire length, but was only active where the high-angle faults turned to follow the path of the pre-existing low-angle fault segment (Fig. 9).

1.7. Possible significance for core-complex geometry

In the Basin and Range major low-angle normal faults are folded into large, broad, periclinal (doubly plunging) antiformal and synformal geometries. The origin of these large-scale warps of the fault zones is controversial. It is uncertain whether they formed during one process, or by two superimposed events. Suggested processes for forming the extension perpendicular warps include: (1) an isostatic response to tectonic denudation (e.g. Rehrig and Reynolds, 1980; Wernicke and Axen, 1988; Buck, 1988), (2) folding due to motion on synchronous or younger structures in the lower plate such as a detachment fault, or a higher angle fault or shear zone (Spencer, 1984; Wernicke, 1985; Lister and Davis, 1989; Reynolds and Lister, 1990), and (3) movement along a ramp–flat fault surface (John, 1987).

The extension-parallel warps are perhaps the most difficult to explain. If they developed separately from the extension perpendicular warps they could represent original corrugations in the fault plane such as those caused by lateral and oblique ramps (Davis and Hardy, 1981; John, 1987). Alternatively synchronous formation of both fold sets may be caused by the following mechanisms: (1) emplacement of syn-tectonic plutons (Reynolds and Lister, 1990), (2) isostatically uncompensated Moho topography (Yin, 1989) and (3) compressive deviatoric stresses perpendicular to the extension direction (Yin and Dunn, 1992).

The Lokichar fault is not located in the typical setting of low-angle normal faults, but it can, perhaps, shed some light on their evolution. The fault plane shows marked along-strike changes in dip amount, which has significance for the flexural isostatic uplift models previously proposed for the formation of low-angle faults (e.g. Wernicke and Axen, 1988; Buck, 1988). The amount of flexural isostatic footwall uplift associated with a fault is a function of both the displacement amount and the dip of the fault (e.g. Kusznir et al., 1995). This statement assumes that the faults create space in the hanging wall where the originally relatively high-density basement rock that occupied the space is replaced by low-density material. Larger displacements and high-angle faults cause more uplift. Consequently if the observed heaves were tripled on the Lokichar fault the creation of core-complex-type uplifts would be concentrated on the originally high-angle portions of the fault plane (e.g. Kusznir et al.,

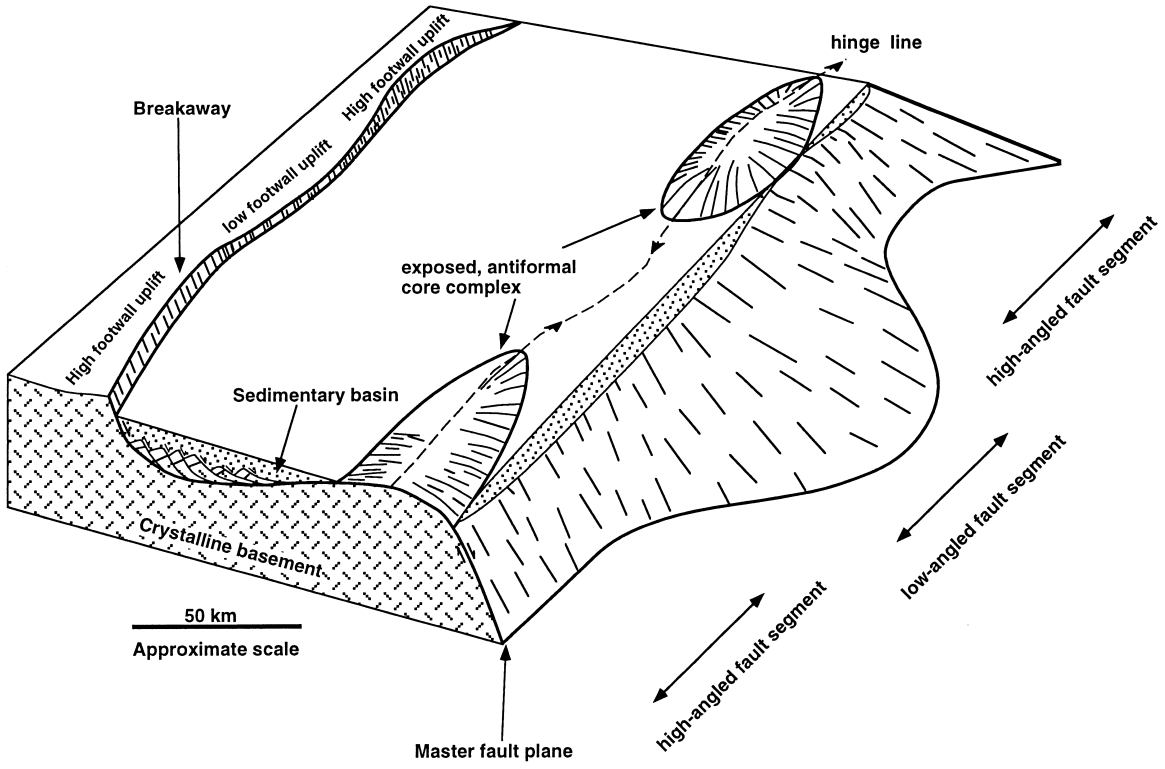

Fig. 10. Schematic block diagram illustrating the relationship between fault angle and rolling hinge footwall uplift, both in the breakaway region and at metamorphic core complexes. Based on isostatic footwall uplift models for core complex formation by Buck (1988) and Wernicke and Axen (1988).

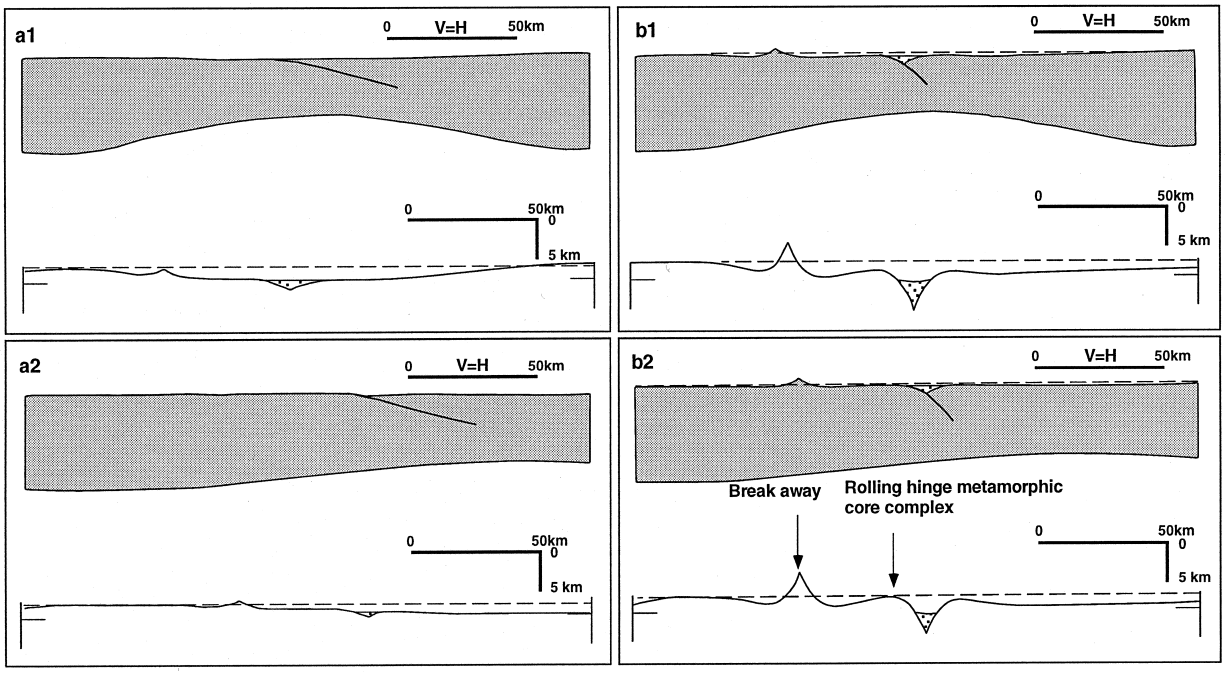

Fig. 11. Stretch model for an initially low-angle (20°) normal fault (a1 and a2) and an initially high-angle (b1 and b2) normal fault. Model parameters: 50 km heave, 50 km initial crustal thickness, 1.5 km effective elastic thickness. In a1 and b1 ductile extension is distributed over 200 km, in a2 and b2 the distance is 300 km.

1995, their fig. 18; Fig. 10), while the low-angle segments would form areas of considerably less uplift. Fig. 11 illustrates this point.

Using the STRETCH model (e.g. Kusznir et al., 1995), 20°- and 60°-dipping faults were modelled with 50 km displacement, in 50 km thick continental crust. The crustal thickness is large, not to match the Kenya rift, but to mimic extension in an orogenic belt, such as the Basin and Range province. It is apparent from the models that much greater footwall uplift is associated with the high-angled fault (Fig. 11). Two other variables that affect the magnitude of the uplifts are the width and location of the ductile stretching zone in the lower crust. Two examples are given for each of the fault dips, in a1 and b1 the 50 km of ductile extension is distributed over 200 km, while in a2 and b2 it is distributed over 300 km. Greater footwall uplift occurs where the ductile stretching is more widely distributed, and/or if the location of the ductile stretching zone is located away from the footwall area, and lies predominantly under the hanging wall. In the examples of 20°-dipping faults, the effects of the ductile stretching geometry on footwall uplift is so strong as to inhibit any antiformal metamorphic core complex geometry from developing. Axen and Bartley (1997) have suggested that sediment loading of the footwall block may also have an inhibiting effect on footwall uplift.

The variations in footwall uplift caused by lateral changes in dip avoids the need to find two-stage mechanisms to generate core complexes or to have pronounced lateral or oblique ramps in the fault plane (e.g. Spencer, 1984; Wernicke, 1985; John, 1987; Lister and Davis, 1989; Reynolds and Lister, 1990). Instead, gradual along-strike changes in dip on the boundary fault could also generate along-strike saddles and highs in a flexurally uplifted footwall (Fig. 10).

2. Conclusions

In East Africa, under normal conditions of rifting, boundary faults tend to be steep, with dips ranging from 45° to 70°. In regions of high heat flow and strong volcanic activity some half graben boundary faults tend to be gentle (30–60°).

Along the Lokichar fault, high-angle fault segments dipping between 30 and 60° pass along strike into very low-angle (12–20°) segments. In other parts of the world, low-angle faults have been explained as a result of pre-existing fabrics or rotation by isostatic adjustment (e.g. Cheadle et al., 1987; Wernicke and Axen, 1988; Buck, 1988). These mechanisms can be ruled out for the Lokichar fault unless the pre-existing fabric is low-angle thrust faults created during the early stages of syn-extension igneous dyke intrusion. The very low-angle segments appear to coincide with areas of most intense igneous intrusion. Re-orientation of regional stresses by the intrusions (Parsons and Thompson, 1993) or by igneous intrusion-triggered ductile flow of the lower crust (Yin, 1989) are possible mechanisms that could have initiated these faults.

The theoretical difficulty of attaining shear stresses high enough to move low-angle normal faults in preference to high-angle faults (e.g. Wills and Buck, 1997) is supported by observations that (1) the low-angle portions of the Lokichar fault are associated with domino-style tilted fault blocks in the hanging wall, while such faults are not seen where the boundary fault is higher angle, and (2) displacement is considerably lower on the low-angle fault segment than the southern high-angle fault segment. Initiation of the low-angle fault segment might have been facilitated by high pore-fluid pressures along the low-angle fault generated during volcanic activity in the area. Subsequent motions might have been concentrated along the high-angle fault segments and the portions of the low-angle fault down-dip of the active high-angle faults (Fig. 9)

In the Basin and Range some major present-day low-angle faults were initiated as high-angle faults (e.g. Wernicke and Axen, 1988). The unstated implication is that such faults were steeply dipping along their entire length. The geometry of the Lokichar fault shows steeply and gently dipping fault segments can exist along the same fault trace, challenging simplistic perceptions of fault correlation. In addition variability in fault dip along strike is one mechanism to explain the metamorphic core complex geometry, since isostatic uplift associated with low-angle fault segments will be less than that along the high-angle segments. This along-strike variation will cause the broad regional undulose geometry of the footwall uplift (Fig. 10). Thus it is a mechanism which can explain the synchronous formation of the two fold (periclinal) orientations found in antiformal metamorphic core complexes.

Flexural modeling of low-angle fault geometries shows that metamorphic core-complex geometries are unlikely to develop along low-angle faults. The width and location of the zone of lower crustal ductile stretching could play a significant role in inhibiting metamorphic core complex (rolling hinge) uplift under gently dipping faults.

Acknowledgements

I would like to thank Amoco for permission to release the data on the Lokichar basin, and Denise Stone, Bob Harper and Bill Wescott who originally worked on the data. The manuscript benefitted greatly from detailed reviews by Gary Axen and Elizabeth Miller.

References

Anderson, E.M., 1951. The Dynamics of Faulting. Oliver and Boyd, Edinburgh.

Axen, G.J., 1992. Pore pressure, strain increase, and fault weakening in low-angle normal faulting. Journal of Geophysical Research 97, 8979–8991.

Axen, G.J., Bartley, J.M., 1997. Field tests of rolling hinges. Journal of Geophysical Research 102, 20515–20537.

Boschetto, H.B., Brown, F.H., McDougall, I., 1992. Stratigraphy of the Lothikok Range, northern Kenya, and K/Ar ages of its Miocene Primates. Journal of Human Evolution 22, 47–71.

Buck, R.W., 1988. Flexural rotation of normal faults. Tectonics 7, 959–973.

Byerlee, J., 1978. Friction of rocks. Pure and Applied Geophysics, 615–625.

Cheadle, M.J., McGeary, S., Warner, M.R., Matthews, D.H., 1987. Extensional structures on the western U.K. continental shelf: a review of evidence from deep seismic profiling. In: Coward, M.P., Dewey, J.F., Hancock, P.L. (Eds.), Continental Extensional Tectonics (special issue). Geological Society of London Special Publication 28, 445–465.

Davis, G.H., Hardy Jr, J.J., 1981. The Eagle Pass detachment, southeastern Arizona—product of mid Miocene normal faulting in the southern Basin and Range. Geological Society of America Bulletin 92, 749–762.

Doser, D.I., Yarwood, D.R., 1994. Deep crustal earthquakes associated with continental rifts. Tectonophysics 229, 123–131.

Dunkleman, T.J., Rosendahl, B.R., Karson, J.A., 1989. Structure and stratigraphy of the Turkana Rift from seismic reflection data. Journal of African Earth Sciences 8, 489–510.

Ebinger, C.J., Rosendahl, B.R., Reynolds, D.J., 1987. Tectonic model of the Malawi rift, Africa. Tectonophysics 141, 215–235.

Gibbs, A.D., 1983. Balanced cross-section construction from seismic sections in areas of extensional tectonics. Journal of Structural Geology 5, 153–160.

Hendrie, D.B., Kusznir, N.J., Morley, C.K., Ebinger, C.J., 1994. A quantitative model of Cenozoic rift basin development in Northern Kenya. Tectonophysics 236, 409–438.

Jackson, J., 1987. Active normal faulting and crustal extension. Coward, M.P., Dewey, J.F., Hancock, P.L. (Eds.) Continental extensional tectonics. Geological Society of London Special Publication 28, 3–17.

John, B.E., 1987. Geometry and evolution of a mid-crustal extensional fault system: Chemehuevi Mountains, southeastern California. Coward, M.P., Dewey, J.F. (Eds.) Continental Extensional Tectonics. Geological Society of London, Special Publication 28, 313–335.

Kusznir, N.J., Marsden, G., Egan, S.S., 1991. A flexural-cantilever simple-shear/pure-shear model of continental lithosphere extension: applications to the Jeanne d'Arc Basin, Grand Banks and Viking Graben, North Sea. Roberts, A.M., Yielding, G., Freeman, B. (Eds.) The Geometry of Normal Faults. Geological Society of London, Special Publication 56, 41–60.

Kusznir, N.J., Roberts, A.M., Morley, C.K., 1995. Forward and reverse modelling of rift basin formation. In: Lambiase, J.J. (Ed.), Hydrocarbon Habitat in Rift Basins (special issue). Geological Society of London, Special Publication 80, 33–56.

Le Van Hung, 1996. Hydrocarbon generation assessment of Lokichar Basin, Kenya. M. Sc. thesis, University of Brunei, Darussalam.

Lister, G.S., Davis, G.A., 1989. The origin of metamorphic core complexes and detachment faults formed during Tertiary continental extension in the northern Colorado River region, U.S.A. Journal of Structural Geology 7, 65–93.

Mechie, J., Keller, G.R., Prodehl, C., Gaciri, S., Braile, L.W., Mooney, W.D., Gajewski, D., Sandmeier, K.-J., 1994. Crustal stucture beneath the Kenya Rift from axial profile data. Tectonophysics 236, 179–200.

Morley, C.K., 1989. Extension, detachments and sedimentation in continental rifts (with particular reference to East Africa). Tectonics 8, 1175–1192.

Morley, C.K., Nelson, R.A., Patton, T.L., Munn, S.G., 1990. Transfer zones in the East African rift system and their relevance to hydrocarbon exploration in rifts. American Association of Petroleum Geologists Bulletin 74, 1234–1253.

Morley, C.K., Wescott, W.A., Stone, D.M., Harper, R.M., Wigger, S.T., Karanja, F.M., 1992. Tectonic evolution of the northern Kenya Rift. Journal of the Geological Society of London 149, 333–348.

Morley, C.K., Wescott, W.A., Stone, D.M., Harper, R.M., Wigger, S.T., Karanja, F.M., Day, R.A., Geology and geophysics of the western Turkana basins. In: Morley, C.K., (Ed.), Continental rifting in East Africa, structural and sedimentary geometries, processes and evolution: as revealed by hydrocarbon exploration. American Association of Petroleum Geologists Special Publication (in press).

Parsons, T., Thompson, G.A., 1993. Does magmatism influence low-angle normal faulting? Geology 21, 247–250.

Proffett Jr, J.M., 1977. Cenozoic geology of the Yerington district, Nevada, and implications for the nature and origin of Basin and Range faulting. Geological Society of America Bulletin 88, 247–266.

Rehrig Jr., W.A., Reynolds, S.J., 1980. Geologic and geochronologic reconnaissance of a northwest trending zone of metamorphic core complexes in southern and western Arizona. Crittenden, M.D., Coney, P.J., Davis, G.H. (Eds). Cordilleran Metamorphic Core Complexes. Memoirs of the Geological Society of America 153, 131–157.

Reynolds, S.J., Lister, G.S., 1990. Folding of mylonite zones in Cordilleran metamorphic core complexes: evidence from near the mylonite front. Geology 18, 216–219.

Rosendahl, B.R., Versfelt, J.W., Scholz, C.A., Buck, J.E., Wood, L.D., 1988. Seismic Atlas of Lake Tanganyika, East Africa (Project PROBE Geophysical Atlas Series, folio 1). Duke University, Durham, NC.

Rubin, A.M., Pollard, D.D., 1988. Dike-induced faulting in rift zones of Iceland and Afar. Geology 16, 413–417.

Scott, R.J., Lister, G.S., 1992. Detachment faults; evidence for a low angled origin. Geology 20, 833–836.

Skarmeta, J., Price, N.J., 1984. Deformation of country rocks by an intrusion in the Sierra de Moreno, northern Chilean Andes. Journal of the Geological Society of London 141, 901–908.

Spencer, J.E., 1984. Role of tectonic denudation in warping and uplift of low-angle normal faults. Geology 12, 95–98.

Wernicke, B., 1985. Uniform sense simple shear of the continental lithosphere. Canadian Journal of Earth Sciences 22, 108–125.

Wernicke, B., Axen, G.J., 1988. On the role of isostacy in the evolution of normal fault systems. Geology 16, 848–851.

Wernicke, B., 1995. Low-angle normal faults and seismicity—a review. Journal of Geophysical Research 100, 20159–20174.

Wills, S., Buck, R.W., 1997. Stress-field rotation and rooted detachment faults: a Coulomb failure analysis. Journal of Geophysical Research 102, 20503–20514.

Yin, A., 1989. Origin of regional rooted low-angle normal faults: a mechanical model and its tectonic implications. Tectonics 8, 469–482.

Yin, A., 1990. Reply. Tectonics 9, 547–549.

Yin, A., Dunn, J.F., 1992. Structural and stratigraphic development of the Whipple–Chemehuevi detachment fault system, southeastern California: implications for the geometric evolution of domal and basinal low-angle normal faults. Geological Society of America Bulletin 104, 659–674.